Stability of a Dual-Spin Spacecraft with a Flexible Momentum Wheel

P. M. BAINUM*
Howard University, Washington, D.C.
AND
P. G. FUECHSEL†
The Johns Hopkins University, Applied Physics Laboratory, Silver Spring, Md.
AND
J. V. FEDOR‡
NASA Goddard Space Flight Center, Greenbelt, Md.

The attitude stability of a dual-spin satellite with damping in the momentum wheel as well as the "despun" portion is analyzed. Wheel energy dissipation is modeled by assuming the wheel can flex with two degrees of freedom relative to the hub. The nonlinear attitude equations are derived for small wheel flexural motion and are a ninth order nonautonomous set. If the main body damper mass and wheel transverse moment of inertia are assumed small when compared with main satellite masses and inertias, an averaging process can be used to determine the zeroth and first order secular perturbations on the behavior of the system nutation angle. From this a general analytic stability criterion is established. A numerical evaluation of this criterion using parameters and measured wheel damping data for the Small Astronomy-A satellite indicates that stability about a zero degree nutation angle is insured by a factor of 128 under normal operating conditions. Numerical integration of the nonlinear equations confirms the analytic results for special cases.

Nomenclature

A, B, C = main body and composite moments of inertia about the $\bar{A}, \bar{B}, \bar{C}$ x, y, z axes.
$\bar{b}_i$ = unit vectors along the x, y, z axes ($i = 1, 2, 3$).
$\bar{b}_i'$ = unit vectors fixed to the nominal plane of the undeflected wheel and rotating with it
C_i = coefficients occurring in the steady state solutions for $\phi_1, \alpha_z, \alpha_x$
H = magnitude of system angular momentum vector $\bar{H}$
I_{bi}, I_{Ri} = moment of inertia of the main body and rotor about the $\bar{b}_i$ axis
K, K_R = nutation damper and rotor spring constants
k, k_R = nutation damper and rotor damping constants
l = height of damper plane above x, z plane
L_i = the applied external torques about the $\bar{b}_i$ axis
M = the mass of the main satellite and the rotor
$\bar{M}$ = the total system mass
m = the pendulum end mass
q, q' = $\bar{B}/\bar{A}; I_{R2}/\bar{A}$
r_0 = the distance from the nominal spin (y) axis to the pendulum hinge point
r_1 = the length of the pendulum
$\bar{r}_i$ = unit vectors directed along the rotor principal axes
s = nominal spin rate of rotor relative to main body
T = kinetic energy
t = time
V = potential energy
x, y, z = principal axes of main satellite
α_x, α_z = rotor deflection angles about the $-\bar{b}_1'$, $\bar{r}_3$, axes, respectively
Γ = $lm/\bar{M}$
γ = the nutation angle, i.e., the angle between the $\bar{b}_2$ axis and $\bar{H}$
λ = $[(B - A)\Omega + I_{R2}s]/A$, in the zeroth-order solution, frequency with which transverse angular velocity components rotate about $\bar{b}_2$ axis
Ω = nominal main body spin rate
ω = in the zeroth-order solution, the value of ω_3 at some reference time
ω_i = angular velocities about the x, y, z axes, respectively
ϕ_1 = nutation damper displacement angle
τ = time constant associated with nutation angle decay

Superscripts

$( )'$ = component in $\bar{b}_i'$ axes system
$(\cdot)$ = differentiation with respect to time

Subscripts

ave = averaged quantity
b_i, i = particular main body axis ($i = 1, 2, 3$)
0 = initial state or equilibrium value

Received October 12, 1971; revision received April 20, 1972. Presented as Paper 71-347 at the AAS/AIAA Astrodynamics Specialists Conference, Ft. Lauderdale, Fla., August 17–19, 1971. The analytic portion of this study was performed while one of the authors (PMB) participated in the NASA/ASEE Summer Faculty Fellowship Program (1970); partial support was also provided by Contract NOw 62-0604-c sponsored by NASA.

Index category: Spacecraft Attitude Dynamics and Control.

* Associate Professor of Aerospace Engineering; also Consulting Engineer, The Johns Hopkins University, Applied Physics Laboratory. Member AIAA.

† Engineer. Member AIAA.

‡ Head, Office of Dynamics Analysis, Stabilization and Control Branch. Member AIAA.

Introduction

THE NASA Goddard Space Flight Center is currently directing the design and development of a series of Small Astronomy Satellites (SAS) whose purpose is to support orbitally based experiments in modern astronomy. The first of these satellites, SAS-A, is a dual-spin spacecraft which has the capability of scanning the entire celestial sphere to determine the relative position and intensity of x-ray emitting sources with respect to the fixed position of the stars. It is important that the attitude of the satellite be precisely known and maintained in order to accurately determine the location of the x-ray emitting sources. The attitude control system for the SAS-A satellite has been designed and developed by the Applied Physics Laboratory of the Johns Hopkins University.

An analysis of the attitude motion and stability of such a dual-spin spacecraft with damping only on the slowly spinning

main part was reported previously.[1] The resulting differential equations of rotational motion when linearized were an autonomous set of fifth-order equations with constant coefficients. Analytical stability criteria were developed using the method of Routh-Hurwitz.

Subsequently it was demonstrated by static and dynamic tests of the SAS-A momentum wheel that there was some energy dissipation in the shaft-momentum wheel assembly. The purpose of this investigation is to incorporate the effects of momentum wheel damping into the rotational equations of motion for the SAS-A spacecraft, and to then investigate the attitude stability. A possible way to model the wheel energy dissipation is to add a spring-mass-dashpot damper to the wheel similar to the model of Mingori.[2] It is then necessary to relate the dissipation of the dashpot damper to that of the shaft-momentum wheel assembly. Another approach used by Sen and Fleisher[3] assumes the wheel can flex with two degrees of freedom with respect to the hub. This latter alternative was selected as a more appropriate model since the results of the momentum wheel tests could be directly used in determining wheel restoring and damping coefficients.

Analysis

The present analysis is based upon the dual-spin attitude control system illustrated in Fig. 1. The elements of this system are: 1) the main part of the spacecraft, essentially a right circular cylinder where the nominal spin axis is the $\bar{b}_2$ body axis, 2) a small momentum wheel or rotor assumed to be connected to the primary part near its center of mass, and whose spin axis is nominally parallel to the $\bar{b}_2$ body axis, and 3) a pendulous-type nutation damper which is attached to the main part and constrained to move in a plane a distance l above the $\bar{b}_1$, $\bar{b}_3$ plane (determined by the body axes perpendicular to the symmetry axis, $\bar{b}_2$). The damper is hinged about a torsion wire support which offers a restoring torque in addition to the dissipative torque associated with the damper motion.[4] In addition the rotor is assumed to have two degrees of flexural freedom with respect to the hub, i.e., the plane of the rotor disc is allowed to deviate through small angular deflections from its nominal orientation which is parallel to the x, z, plane.

Equations of Motion

The development of the equations of motion follows that of Ref. 1, except now it is necessary to reformulate the expression for the kinetic energy of the rotor. The rotor is assumed to be spinning with a nominal relative angular velocity magnitude, s, with respect to the main spacecraft. The nominal

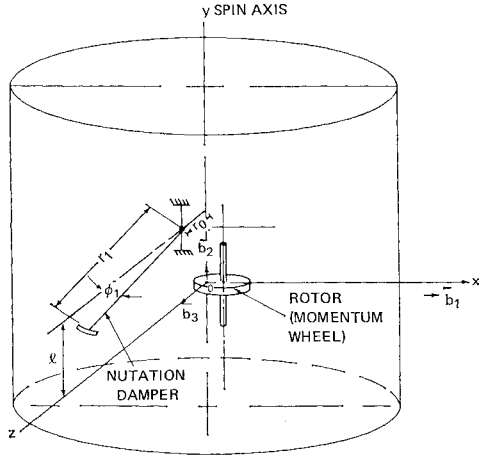

Fig. 1 Elements of SAS-A attitude control system.

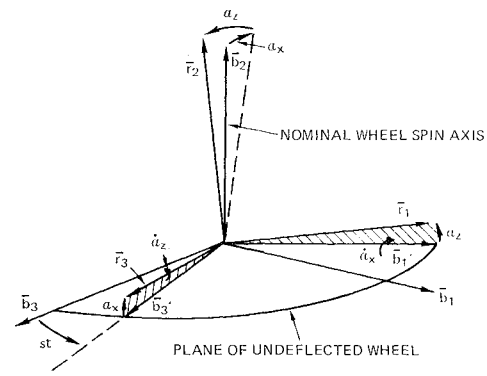

Fig. 2 Momentum wheel deflection geometry.

direction of the rotor spin axis is the direction of the $\bar{b}_2$ unit vector.

We will assume that the $\bar{b}_1'$, $\bar{b}_2'$, $\bar{b}_3'$ unit vectors can be related to the $\bar{r}_1$, $\bar{r}_2$, $\bar{r}_3$ unit vectors along the rotor principal axes by a specific Euler angle sequence (Fig. 2). The $\bar{b}_1'$, $\bar{b}_3'$ unit vectors lie in the plane of the undeflected rotor and rotate with angular velocity, s, relative to the $\bar{b}_1$, $\bar{b}_2$, $\bar{b}_3$ system. The rotation sequence assumes first a rotation through α_x about $-\bar{b}_1'$ and then α_z about $\bar{r}_3$. The $\bar{r}_1$, $\bar{r}_2$, $\bar{r}_3$ fixed in the rotor can then be related to $\bar{b}_1'$, $\bar{b}_2'$, $\bar{b}_3'$ by

$$\begin{aligned}\bar{r}_1 &= \bar{b}_1'\cos\alpha_z + \bar{b}_2'\sin\alpha_z\cos\alpha_x - \bar{b}_3'\sin\alpha_z\sin\alpha_x\\ \bar{r}_2 &= -\bar{b}_1'\sin\alpha_z + \bar{b}_2'\cos\alpha_z\cos\alpha_x - \bar{b}_3'\cos\alpha_z\sin\alpha_x\\ \bar{r}_3 &= \bar{b}_2'\sin\alpha_x + \bar{b}_3'\cos\alpha_x\end{aligned} \tag{1}$$

If $\mathbf{I}$ is the rotor inertia dyadic and $\bar{\omega}_R$ is the inertial angular velocity of the rotor then

$$T_{\text{rotor}} = \tfrac{1}{2}\bar{\omega}_R\cdot\mathbf{I}\cdot\bar{\omega}_R \tag{2}$$

and

$$\mathbf{I} = I_{R_1}\bar{r}_1\bar{r}_1 + I_{R_2}\bar{r}_2\bar{r}_2 + I_{R_1}\bar{r}_3\bar{r}_3 \tag{3}$$

for an assumed symmetric rotor. The angular velocity of the rotor has contributions due to the undeflected wheel rates plus deflection rates according to

$$\begin{aligned}\bar{\omega}_R = {}&(\omega_1' - \dot{\alpha}_x)\bar{b}_1' +\\ &(\omega_2' + \dot{\alpha}_z\sin\alpha_x)\bar{b}_2' + (\omega_3' + \dot{\alpha}_z\cos\alpha_x)\bar{b}_3'\end{aligned} \tag{4}$$

From Eqs. (1) and (4),

$$\begin{aligned}\bar{\omega}_R = {}&[(\omega_1' - \dot{\alpha}_x)\cos\alpha_z + (\omega_2' + \dot{\alpha}_z\sin\alpha_x)\cos\alpha_x\sin\alpha_z -\\ &(\omega_3' + \dot{\alpha}_z\cos\alpha_x)\sin\alpha_x\sin\alpha_z]\bar{r}_1 +\\ &[-(\omega_1' - \dot{\alpha}_x)\sin\alpha_z + (\omega_2' - \dot{\alpha}_z\sin\alpha_x)\cos\alpha_x\cos\alpha_z -\\ &(\omega_3' + \dot{\alpha}_z\cos\alpha_x)\sin\alpha_x\cos\alpha_z]\bar{r}_2 +\\ &[(\omega_2' + \dot{\alpha}_z\sin\alpha_x)\sin\alpha_x + (\omega_3' + \dot{\alpha}_z\cos\alpha_x)\cos\alpha_x]\bar{r}_3\end{aligned} \tag{5}$$

We can also define,

$$\bar{\omega}_R \equiv \omega_{r_1}\bar{r}_1 + \omega_{r_2}\bar{r}_2 + \omega_{r_3}\bar{r}_3 \tag{6}$$

From Eqs. (2, 3, and 6), the rotor kinetic energy may be expressed by

$$T_{\text{rotor}} = \tfrac{1}{2}I_{R_1}\omega_{r_1}^2 + \tfrac{1}{2}I_{R_2}\omega_{r_2}^2 + \tfrac{1}{2}I_{R_1}\omega_{r_3}^2 \tag{7}$$

After substituting Eq. (5) into Eq. (7) and neglecting terms above the second degree in ω_1', ω_3', α_x, α_z, $\dot{\alpha}_x$, $\dot{\alpha}_z$, a quadratic approximation for T_{rotor} may be obtained:

$$\begin{aligned}&T_{\text{rotor}}\\ &= \tfrac{1}{2}I_{R_1}[\omega_1'^2 - 2\omega_1\dot{\alpha}_x + \dot{\alpha}_x^2 + 2\omega_2'\alpha_z(\omega_1' - \dot{\alpha}_x) + (\omega_2'\alpha_z)^2] +\\ &\tfrac{1}{2}I_{R_2}[\omega_2'^2 + 2\omega_2'(-\alpha_x\omega_3' - \alpha_z\omega_1' + \alpha_z\dot{\alpha}_x) -\\ &\omega_2'^2(\alpha_x^2 + \alpha_z^2)] +\\ &\tfrac{1}{2}I_{R_1}[\omega_3'^2 + 2\omega_3'\dot{\alpha}_z + \dot{\alpha}_z^2 + 2\omega_2'\alpha_x(\omega_3' + \dot{\alpha}_z) + (\omega_2'\alpha_x)^2]\end{aligned} \tag{8}$$

For a homogeneous symmetrical rotor, $I_{R_2} = 2I_{R_1}$. By writing the ω_i' in terms of the ω_i (Fig. 2), Eq. (8) may be expanded in terms of the spacecraft body angular rates to yield

$$T_{\text{rotor}} = I_{R_1}(\omega_2 + s)^2 + \tfrac{1}{2}I_{R_1}(\omega_1^2 + \omega_3^2) + (I_{R_1}/2)[2\dot{\alpha}_z(\omega_3 \cos st + \omega_1 \sin st) - 2\dot{\alpha}_x(-\omega_3 \sin st + \omega_1 \cos st) - 2(-\omega_3 \sin st + \omega_1 \cos st)(\omega_2 + s)\alpha_z - 2(\omega_3 \cos st + \omega_1 \sin st)(\omega_2 + s)\alpha_x + 2(\omega_2 + s)(\alpha_x\dot{\alpha}_z + \alpha_z\dot{\alpha}_x) - (\omega_2 + s)^2(\alpha_z^2 + \alpha_x^2) + \dot{\alpha}_z^2 + \dot{\alpha}_x^2] \quad (9)$$

If it is now assumed that the wheel dissipative forces vary linearly with the flexural angular rates $\dot{\alpha}_x$ and $\dot{\alpha}_z$, these forces can be derived from a Rayleigh dissipation function $\mathcal{F}$ similar to that given in Ref. 1, which has the form:

$$\mathcal{F} = \tfrac{1}{2}[k_1\dot{\phi}_1^2 + k_R(\dot{\alpha}_x^2 + \dot{\alpha}_z^2)] \quad (10)$$

where k_R is the equivalent linear viscous damping constant of the rotor. Wheel damping tests performed at the Applied Physics Laboratory verify that, to first order, there is a linear relationship between wheel dissipative forces and the flexural angular rates. (Likins et al.[5] have recently discussed some of the difficulties which can result due to damping nonlinearities in dual spin systems and have also presented a technique of relating an equivalent linear viscous damping coefficient to the actual nonlinear damping.)

In addition to the restoring torque supplied by the torsion wire support[1,4] of the damper, there is also a restoring effect due to the stiffness of the rotor material itself. For small deflections and homogeneous wheel material these forces can be obtained from the following potential energy expression:

$$V_{\text{rotor}} = \tfrac{1}{2}K_R(\alpha_z^2 + \alpha_x^2) \quad (11)$$

where K_R is the restoring spring constant of the rotor and dependent on the EI_R of the rotor material. The complete potential energy for the system now can be expressed as:

$$V = \tfrac{1}{2}[K\phi_1^2 + K_R(\alpha_z^2 + \alpha_x^2)] \quad (12)$$

whereas the complete rotational kinetic energy for the system is the sum of main body, nutation damper, and rotor components:

$$T = T_M + T_m + T_R \quad (13)$$

and the rather lengthy expression for $T_M + T_m$ is presented in Ref. 1 (in report form).

From the Lagrangian

$$L = T - V \quad (14)$$

the equations of motion for the system can be expressed in terms of the quasicoordinates $(\omega_1, \omega_2, \omega_3)$, the angle swept out by the pendulous nutation damper (ϕ_1), and the rotor deflection angles (α_x, α_z) according to Ref. 1 and 6. Numerical studies with the previously developed nonlinear equations of motion[1] indicate that whenever the transverse components of main body angular velocities are the same order as ω_2, the nutation damper motion is characterized by large amplitudes and eventually makes contact with the mechanical stops limiting ϕ_1 amplitudes to $\pm 20°$. Because a stability analysis of such a discontinuous system is beyond the scope of the present analysis, it was decided to expand the equations under the assumptions that $\omega_i < \omega_2$, $\dot{\alpha}_{x,z} < \omega_2$, $\dot{\phi}_1 < \omega_2$, $\phi_1 < 1$, and $\alpha_{x,z} < 1$. The following first order nonlinear equations of motion result:

$$\bar{B}\dot{\omega}_2 + \omega_1\omega_3(\bar{A} - \bar{C}) + mr_1(r_1 + r_0)\ddot{\phi}_1 = L_2 \quad (15)$$

$$\bar{A}\dot{\omega}_1 + \omega_2\omega_3(\bar{C} - \bar{B}) - \omega_3 I_{R_2}s - 2m\omega_2 r_1(lM/\bar{M})\dot{\phi}_1 + I_{R_1}\{[\ddot{\alpha}_z + (\omega_2 + s)^2\alpha_z]\sin st - [\ddot{\alpha}_x + (\omega_2 + s)^2\alpha_x]\cos st\} = L_1 \quad (16)$$

$$\bar{C}\dot{\omega}_3 + \omega_1\omega_2(\bar{B} - \bar{A}) + \omega_1 I_{R_2}s - mr_1(lM/\bar{M})\ddot{\phi}_1 + m\omega_2^2 r_1 \times (lM/\bar{M})\phi_1 + I_{R_1}\{[\ddot{\alpha}_z + (\omega_2 + s)^2\alpha_z]\cos st + [\ddot{\alpha}_x + (\omega_2 + s)^2\alpha_x]\sin st\} = L_3 \quad (17)$$

$$mr_1^2\left(1 - \frac{m}{\bar{M}}\right)\ddot{\phi}_1 - mr_1\frac{lM}{\bar{M}}\dot{\omega}_3 + mr_1(r_0 + r_1) \times \dot{\omega}_2 + \omega_2^2 mr_1\left(r_0 + \frac{mr_1}{\bar{M}}\right)\phi_1 + m\omega_2 r_1\frac{lM\omega_1}{\bar{M}} = -k\dot{\phi}_1 - K\phi_1 \quad (18)$$

$$I_{R_1}\ddot{\alpha}_z + k_R\dot{\alpha}_z + [K_R + I_{R_1}(\omega_2 + s)^2]\alpha_z + I_{R_1}\{[\dot{\omega}_1 - (\omega_2 + 2s)\omega_3]\sin st + [\dot{\omega}_3 + (\omega_2 + 2s)\omega_1]\cos st\} = 0 \quad (19)$$

$$I_{R_1}\ddot{\alpha}_x + k_R\dot{\alpha}_x + [K_R + I_{R_1}(\omega_2 + s)^2]\alpha_x + I_{R_1}\{[\dot{\omega}_3 + (\omega_2 + 2s)\omega_1]\sin st - [\dot{\omega}_1 - (\omega_2 + 2s)\omega_3]\cos st\} = 0 \quad (20)$$

For small displacements of the nutation damper, and for $m/M \ll 1$, the lateral center of mass shift due to this motion will be very small and is not included in these equations. It is assumed, of course, that the satellite is statically balanced in equilibrium when $\phi_1 = 0$. For the case where $I_{R_2} \neq 2I_{R_1}$, additional first order terms will appear in the deflection equations which will become dynamically coupled in deflection rates.

Stability Criteria

Equations (15–20) when linearized about the equilibrium motion: $\omega_2 = \Omega, \omega_1 = \omega_3 = \phi_1 = \alpha_x = \alpha_z = \dot{\omega}_1 = \dot{\omega}_3 = \dot{\phi}_1 = \dot{\alpha}_x = \dot{\alpha}_z = 0$ would represent a set of nonautonomous differential equations with both constant and periodic coefficients. The stability of such a system could be analyzed using Floquet theory similar to the treatment of Mingori.[2] In an effort to analyze the stability of this system, the technique employed by Flatley,[7] was applied.

It is assumed that the effects of the nutation damper and wheel deflections relative to the hub are small perturbations on the nominal rigid body motion of the torque-free dual-spin system. The "zeroth-order" equations which represent the reference motion, or unperturbed state, can be obtained by assuming that terms such as mr_1^2 and $mr_1 l$ are much smaller than main body inertia terms A, B, and C, and also that $I_{R_1} \ll A, B,$ or C. The SAS-A satellite is almost perfectly symmetrical about the $\bar{b}_2$ axis so that $A = C$; also under the approximations mentioned above $A = \bar{A}$, $B = \bar{B}$. The resulting zeroth order equations corresponding to Eqs. (15–17) with $L_i = 0$ are

$$B\dot{\omega}_2 = 0 \quad (21)$$

$$A\dot{\omega}_1 - \omega_2\omega_3(B - A) - \omega_3 I_{R_2}s = 0 \quad (22)$$

$$A\dot{\omega}_3 + \omega_1\omega_2(B - A) + \omega_1 I_{R_2}s = 0 \quad (23)$$

Eq. (21) has the solution $\omega_2 = \Omega$, which when substituted into Eqs. (22) and (23) yields:

$$\omega_1 - \lambda\omega_3 = 0 \quad (24)$$

$$\omega_3 + \lambda\omega_1 = 0 \quad (25)$$

The solution to Eqs. (24) and (25) has the form

$$\omega_1 = \omega \sin\lambda t \quad (26)$$

$$\omega_3 = \omega \cos\lambda t \quad (27)$$

where $\omega = \omega_3(0)$, the value at some reference time. If $s = 0$, the system reduces to the classical problem of the spinning symmetrical rigid body.

To determine the first order damper and wheel deflection motions all terms linear in m and I_{R_1} are retained. After

substitution of the zeroth order main body angular velocities into the equations for the damper and wheel deflections the following equations result:

$$mr_1^2\ddot{\phi}_1 + k\dot{\phi}_1 + (K + mr_1r_0\Omega^2)\phi_1 = -mr_1\Gamma\omega[(\lambda + \Omega)\sin\lambda t] \quad (28)$$

$$I_{R_1}\ddot{\alpha}_z + k_R\dot{\alpha}_z + [K_R + I_{R_1}(s + \Omega)^2]\alpha_z = -I_{R_1}\omega \times [(\lambda - \Omega - 2s)\sin(s - \lambda)t] \quad (29)$$

$$I_{R_1}\ddot{\alpha}_x + k_R\dot{\alpha}_x + [K_R + I_{R_1}(s + \Omega)^2]\alpha_x = I_{R_1}\omega[(\lambda - \Omega - 2s)\cos(s - \lambda)t] \quad (30)$$

Equations (29) and (30) correspond identically to the approximate wheel deflection equations derived previously.[3]

The steady-state solutions to Eqs. (28-30) can be written in the form

$$\phi_{1_{ss}} = C_1\sin\lambda t + C_2\cos\lambda t \quad (31)$$

$$\alpha_z = C_3\sin(s - \lambda)t + C_4\cos(s - \lambda)t \quad (32)$$

$$\alpha_x = C_5\sin(s - \lambda)t + C_6\cos(s - \lambda)t \quad (33)$$

where

$$D_1C_1 = -mr_1\Gamma\omega(\lambda + \Omega)[K + mr_1(r_0\Omega^2 - r_1\lambda^2)]$$
$$D_1C_2 = mr_1\Gamma k\omega\lambda(\lambda + \Omega)$$
$$D_2C_3 = -I_{R_1}\omega(\lambda - \Omega - 2s)\{K_R + I_{R_1}[(s + \Omega)^2 - (s - \lambda)^2]\}$$
$$D_2C_4 = I_{R_1}\omega(\lambda - \Omega - 2s)(s - \lambda)k_R;\ C_5 = C_4;\ C_6 = -C_3$$
$$D_1 = [K + mr_1(r_0\Omega^2 - r_1\lambda^2)]^2 + (k\lambda)^2$$
$$D_2 = \{K_R + I_{R_1}[(s + \Omega)^2 - (s - \lambda)^2]\}^2 + (s - \lambda)^2k_R^2$$

In the absence of the external torques the total angular momentum vector of the system about an axis passing through the system center of mass (point 0) remains time invariant. If the nutation angle, γ, is defined as the angle between the $\bar{b}_2$ axis and the total angular momentum vector of the system, $\bar{H}$, then

$$H_2 = \cos\gamma \quad (34)$$

The component H_2 may be obtained from

$$H_2 = B\omega_2 + (\bar{r}_{m0} \times \bar{P}_{m0}) \cdot \bar{b}_2 + \bar{H}_{\text{rotor}} \cdot \bar{b}_2 \quad (35)$$

where $\bar{P}_{m0}$ is the linear momentum of the nutation damper about an axis through 0, and $\bar{r}_{m0}$ is the position vector of the pendulum end mass. After expansion of Eq. (35) and neglecting terms involving $m^2/\bar{M} \ll m$

$$H_2 = B\omega_2 + m\{(r_1^2 + r_0^2 + 2r_0r_1\cos\phi_1)(\omega_2 + \dot{\phi}_1) + \Gamma[-\omega_1r_1\sin\phi_1 - \omega_3(r_0 + r_1\cos\phi_1)] - \dot{\phi}_1(r_0^2 + r_1r_0\cos\phi_1)\} + I_{R_2}(\omega_2 + s) - I_{R_1}(\omega_2 + s)(\alpha_z^2 + \alpha_x^2) - I_{R_1}[\alpha_z(-\omega_3\sin st + \omega_1\cos st) + \alpha_x(\omega_3\cos st + \omega_1\sin st)] + I_{R_1}(\alpha_x\dot{\alpha}_z + \alpha_z\dot{\alpha}_x) \quad (36)$$

By differentiating both sides of Eq. (36) with respect to time, and substituting for $\dot{\omega}_2$ from the higher order nonlinear form of Eq. (15), the following expression is obtained for $\dot{H}_2$:

$$-H\sin\gamma\dot{\gamma} = -mr_0r_1\dot{\phi}_1^2\sin\phi_1 + m\Gamma r_1[\omega_2\omega_3\sin\phi_1 - \omega_2\omega_1\cos\phi_1 + \dot{\phi}_1 \times (-\omega_1\cos\phi_1 + \omega_3\sin\phi_1)] + I_{R_1}\{[\omega_3\cos st + \omega_1\sin st][\alpha_z(\omega_2 + s) + \dot{\alpha}_x] + [\omega_3\sin st - \omega_1\cos st][\alpha_x(\omega_2 + s) - \dot{\alpha}_z]\} \quad (37)$$

Eq. (37) is an exact expression except for the limitation on the magnitudes of M and α_z, α_z. If $m = I_{R_1} = 0$, the cone angle γ is a constant of the motion. To analytically express the first order perturbation of the cone angle, the zeroth-order expressions for main body rates are first substituted into Eq. (37). Then, substitution for α_z and α_x, Eqs. (32) and (33), would produce $\sin^2$ and $\cos^2$ terms in $(s - \lambda)t$, while substitution of ϕ_1, Eq. (31), would produce $\sin^2$ and $\cos^2$ terms and higher order terms in λt, after the $\sin\phi_1$ and $\cos\phi_1$ terms have been expressed in series form. With the use of trigonometric identities, the squared terms may be eliminated, the higher order terms reduced, so that the resulting equation would contain only constants and sinusoidal oscillatory terms.

Following Flatley,[7] the systematic change of γ is considered to be influenced mainly by the constant terms, with the sinusoidal terms contributing only small perturbations of γ about some average value. After retaining only the constant terms in the averaging process, the secular motion of the nutation angle can be described by

$$\dot{\gamma} = -(\omega/2H\sin\gamma) \times [mr_1\Gamma(\Omega + \lambda)C_2 + I_{R_1}(2s - \lambda + \Omega)(C_4 + C_5)] \quad (38)$$

Substituting the values of C_2, C_4, and C_5 from Eq. (31-33), and approximating $H\sin\gamma$ by the transverse angular momentum of the unperturbed motion, Eq. (38) becomes

$$\dot{\gamma} = -\frac{H\sin\gamma}{2A^2}\left[\frac{(mr_1\Gamma)^2(\Omega + \lambda)^2k\lambda}{D_1} - \frac{2I_{R_1}^2(2s - \lambda + \Omega)^2k_R(s - \lambda)}{D_2}\right] \quad (39)$$

where $\omega = H\sin\gamma/A$; $\Omega = [H\cos\gamma - I_{R_2}s]/B$ and $\lambda = [(B - A)H\cos\gamma + AI_{R_2}s]/BA$. Equation (39) has the form $\dot{\gamma} = f(\gamma)$, and equilibrium will be possible whenever $f(\gamma) = 0$. Stability at an equilibrium point, γ_0, requires $f(\gamma_0) = 0$ and $df/d\gamma|_{\gamma_0} < 0$. Thus, the attitude behavior of this ninth order, nonlinear system is represented by this single first-order differential equation, Eq. (39).

If $\dot{\gamma} = f(\gamma) = F(\gamma)\sin\gamma$, then an equilibrium state will always exist at $\gamma_0 = 0$, $\gamma_0 = \pi$, and, possibly at intermediate nutation angles, if $F(\gamma_0) \equiv 0$. For this application the nutation angle is bounded by $0 \leq \gamma \leq \pi$. For stability, from consideration of $f'(\gamma_0) < 0$, at $\gamma_0 = 0$, it is necessary that $F(0) < 0$; at $\gamma_0 = \pi$, it is necessary that $F(\pi) > 0$; at γ_0, it is necessary that, $F(\gamma_0) = 0$ and $F'(\gamma_0) < 0$.

Special Case-Damper on Spacecraft Only

For the case where there is only damping present on the main part of the spacecraft and no damping on the wheel

$$F = -H[(mr_1\Gamma)^2(\Omega + \lambda)^2k\lambda]/2A^2D_1 \quad (40)$$

When $k = 0$, or $l = \Gamma = 0$, or $r_1 = 0$, then $F = 0$ and the system is unstable for all values of γ_0. The conditions that, for stability at $\gamma_0 = 0$, $k > 0$, $l > 0$, $r_1 > 0$ are part of the necessary and sufficient stability criteria previously derived by the methods of Routh-Hurwitz for the case of spacecraft damping only.[1] Assuming these conditions are satisfied, the sign of F is clearly determined by the sign of $-\lambda$. Therefore, for stability at $\gamma_0 = 0$, $-\lambda < 0$, or $\lambda > 0$, or

$$\lambda|_{\gamma_0=0} = [(B - A)H_{\gamma_0} + AI_{R_2}s]/AB > 0 \quad (41)$$

Condition (41) can be shown to be equivalent to

$$\bar{B} + I_{R_2}(s/\Omega) - \bar{A} > 0 \quad (42)$$

within the assumptions previously made regarding A, $\bar{A}$, and B, $\bar{B}$. Inequality (42) is equivalent to inequality (16) of Ref. 1, resulting from the Routh-Hurwitz analysis.

From consideration of Eq. (40), the necessary and sufficient stability criterion, (18), of Ref. 1, repeated here

$$r_0/r_1 + m/\bar{M} + K/mr_1^2\Omega^2 > m\Gamma^2/(\bar{B} - \bar{A} + I_RI_{R_2}s/\Omega) \quad (43)$$

is not apparent.

This can possibly be explained by the fact that m/M and $m\Gamma^2$ (for small or moderate l) are higher order terms when compared with A, B, or $I_{R_2}s/\Omega$ as in the present analysis. In practical application, condition (43) limits the maximum

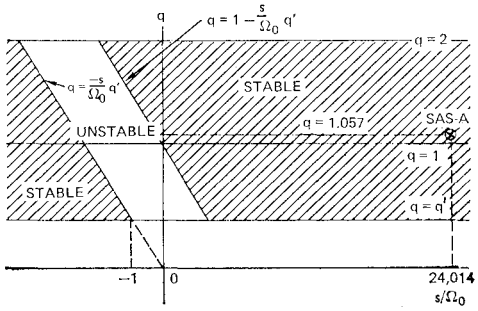

Fig. 3 Stability diagram in q, s/Ω_0 space with damping only on the spacecraft.

height of the damper plane for a given set of main body inertias, nutation damping system parameters, and ratio of s/Ω.

From consideration of inequality (41), the line $\lambda_0 = 0$ or $s/\Omega_0 = (A - B)/I_{R_2}$, divides the initial state plane into the regions $\lambda_0 > 0$, $\lambda_0 < 0$. The region: $\lambda_0 > 0$ is stabilizing for values of $\gamma_0 = 0$, whereas the region: $\lambda_0 < 0$ describes stability for $\gamma_0 = \pi$. Furthermore, the line $B\Omega_0 + I_{R_2}s = H\cos\gamma = 0$ divides the (Ω_0,s) plane into regions describing $\gamma_0 = 0$, and $\gamma_0 = \pi$. Superimposing the two results a stability diagram can be constructed in the (Ω_0,s) plane similar to those shown in Refs. 2 and 7.

A useful alternate form[7] of this stability diagram is obtained by letting: $q = \bar{B}/\bar{A} \approx B/A$, and $q' = I_{R_2}/\bar{A} \approx I_{R_2}/A$. The boundary line, $s/\Omega_0 = (A - B)/I_{R_2}$ becomes $1 = q + q's/\Omega_0$ and the boundary line; $B\Omega_0 + I_{R_2}s = 0$ becomes $q + q's/\Omega_0 = 0$. The transformed stability diagram appears in Fig. 3, where the physically meaningful values of q are restricted to $q' < q < 2$. Unless the momentum wheel is deliberately designed to spin opposite to the sense of the main body angular momentum vector, the physically meaningful values of s/Ω_0 are to the right of the q axis. Figure 3 is identical to a result obtained by Mingori[2] using some of the Routhian stability boundaries.

Special Case-Damper on Momentum Wheel Only

If there is only damping present on the momentum wheel

$$F = H[I_{R_1}{}^2(2s - \lambda + \Omega)^2 k_R(s - \lambda)]/A^2 D_2 \qquad (44)$$

where $k_R = 0$, then $F = 0$, and the system is unstable for all values of γ_0. For this special case, if $k_R > 0$ and there is damping on the wheel, the sign of F is directly dependent on the sign of $(s - \lambda)$. As in the case of damping only on the spacecraft, stability diagrams may be constructed in the (Ω_0,s) plane and also in terms of q and s/Ω_0. The latter diagram is shown in Fig. 4.

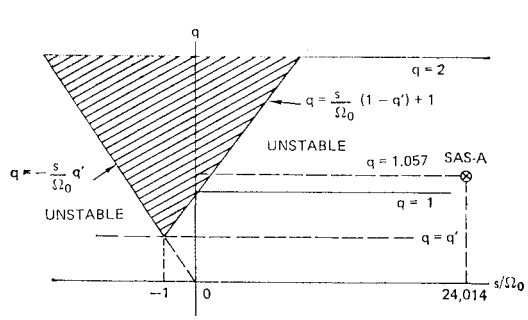

Fig. 4 Stability diagram in q, s/Ω_0 space with damping only on the wheel.

Discussion of General Case

The general expression for time rate of change of nutation angle, (39), may be expressed as:

$$\dot{\gamma} = \frac{\omega^2}{2H\sin\gamma}\left[\frac{-(mr_1\Gamma)^2(\Omega + \lambda)^2 k\lambda}{D_1} + \frac{2I_{R_1}{}^2(2s - \lambda + \Omega)^2 k_R(s - \lambda)}{D_2}\right] \qquad (45)$$

after substituting $1/A^2 = \omega^2/H^2\sin^2\gamma$. From this, necessary conditions for stability at the equilibrium positions of $\gamma_0 = 0$, and $\gamma_0 = \pi$ may be obtained by examining the sign of $F(\gamma_0)$, and at an intermediate position, γ_0, by examining the sign of $F'(\gamma_0)$ as explained earlier.

Likins[8] has derived stability criteria for a dual-spin spacecraft in terms of the average energy dissipation rates on both the wheel and the despun portion using an energy sink analysis. In an effort to compare the form of Eq. (45) with Likins' criteria the average energy dissipation rates were evaluated.

The average energy dissipation rate due to the action of the pendulous nutation damper is developed from Eq. (31) as

$$\dot{T}_{D_{ave}} = -k\dot{\phi}_{1_{ss_{ave}}}{}^2 = \lambda^2(C_1{}^2\cos^2\lambda t - C_1C_2\sin 2\lambda t + C_2{}^2\sin^2\lambda t) \qquad (46)$$

Equation (46) is averaged using the same procedure as before and retaining only the constant terms resulting in

$$\dot{T}_{D_{ave}} = -\lambda^2(mr_1\Gamma)^2\omega^2(\lambda + \Omega)k/2D_1 \qquad (47)$$

Similarly for the rotor, the average energy dissipation rate is the sum of the two components of average dissipation rates

$$\dot{T}_{R_{ave}} = \dot{T}_{R_{z_{ave}}} + \dot{T}_{R_{x_{ave}}} = -k_R(\dot{\alpha}_{x_{ave}}{}^2 + \dot{\alpha}_{z_{ave}}{}^2) \qquad (48)$$

Following the same procedure, it can be shown that

$$\dot{T}_{R_{ave}} = -(s - \lambda)^2 I_{R_1}{}^2\omega^2(\lambda - \Omega - 2s)^2 k_R/D_2 \qquad (49)$$

By comparison of Eqs. (45, 47, and 49), it can be seen that $\dot{\gamma}$ can be written in terms of $\dot{T}_{R_{ave}}$ and $\dot{T}_{D_{ave}}$, as follows:

$$\dot{\gamma} = (1H\sin\gamma)[\dot{T}_{D_{ave}}/\lambda + \dot{T}_{R_{ave}}/(\lambda - s)] \qquad (50)$$

The terms within the bracket of Eq. (50) are identical in form to those appearing in Ref. 8. As Likins indicates the terms $\dot{T}_{D_{ave}}/\lambda$ and $\dot{T}_{R_{ave}}/(\lambda - s)$ are the "first approximation" dissipative torques about the spin axis of the main body and spin axis of the rotor, respectively. The implication here is that if the averaging technique of Flatley[7] were carried to a higher order, additional terms may result in $F(\gamma)$, yielding additional, more complete stability information.

Numerical Results

Calculation of Stability Criteria for SAS-A

For stability, from consideration of $f'(\gamma_0) < 0$, at $\gamma_0 = 0°$ it was necessary that $F(0)$ be numerically evaluated using representative early design SAS-A parameters as follows: $A = 27.0$ kg − m^2; $B = 28.54$ kg-m^2; $I_{R_2} = 2I_{R_1} = 0.011519$ kg-m^2; $m = 0.2158$ kg; $\Gamma = 0.44$ m; $r_0 = 0.019$ m; $r_1 = 0.1833$ m; $\Omega = 0.00872$ rad/sec; $k = 7.0 \times 10^{-5}$ Nt-m-sec/rad; $K = 6.1 \times 10^{-5}$ Nt-m/rad; $K_R = 71.6107$ Nt-m/rad;§ $k_R = 0.006779$ Nt-m-sec/rad.§

Four different values of s were considered: 0, 0.1 nominal, 0.5 nominal and the nominal value of 209.4 rad/sec. We write $F(\gamma)$ as

$$F(\gamma) = H[Q_1 + Q_2]/2A^2 \qquad (51)$$

§ Determined experimentally at The Applied Physics Laboratory, Johns Hopkins University.

Table 1 Stability criteria for SAS-A satellite

s/Ω_0	$Q_1(0)$	$Q_2(0)$	$2A^2/H \cdot F(0)$
0	-2.448×10^{-7}	-2.949×10^{-18}	-2.448×10^{-7}
2,401.3	-1.8379×10^{-5}	3.2185×10^{-6}	-1.516×10^{-6}
12,006.88	-1.3167×10^{-3}	4.015×10^{-4}	-0.9152×10^{-3}
24,013.7615	-0.4092	3.195×10^{-3}	-0.406

where

$$Q_1 = -[(mr_1\Gamma)^2(\Omega+\lambda)^2k\lambda]/D_1$$

and

$$Q_2 = [2I_{R_1}{}^2(2s-\lambda+\Omega)^2k_R(s-\lambda)]/D_2$$

The results are summarized in Table 1.

The system is stable for all four values of s/Ω_0, but the margin of stability for the two intermediate values of s/Ω_0 is not as great as at the nominal operating condition where the stability is insured by a factor of 128. This calculation does not guarantee the system stability during the actual spin-up process, but does give an indication of stability if, for some reason, the wheel does not reach its nominal operating angular velocity, s. The sign change of $Q_2(0)$ verifies that only at very low values of s/Ω_0, is the effect of wheel damping stabilizing. The "X" appearing on the stability charts, Figs. 3 and 4, refers to the SAS-A satellite under nominal operating conditions.

Calculation of Time Constant

Equation (39) has the form $\dot{\gamma}=f(\gamma)$ and at an initial point of equilibrium, $\gamma_0, f(\gamma_0)=0$. If we let $\gamma=\gamma_0+x$ where x is small when compared with γ_0, then $\dot{\gamma}=\dot{x}$, and $f(\gamma_0)+xf'(\gamma_0)\approx f(\gamma)$.

Thus, $\dot{x}\approx xf'(\gamma_0)$ and $dx/x=f'(\gamma_0)\,dt$. This differential equation has the exponential solution of the form: $x=x(0)e^{f'(\gamma_0)t}=x(0)e^{t/\tau}$ where τ is the exponential time constant, and $\tau=-1/f'(\gamma_0)$.

For SAS-A we are interested in the time constant associated with nutation angle decay for an initial equilibrium nutation angle of zero degrees. At $\gamma_0=0$, $f'(0)=F(0)$, and $\tau=-1/F(0)$. Using SAS-A parameters it was found that $\tau=22.3$ min, which compares favorably with previous numerical integration results not including wheel damping.[1]

Results of Numerical Integration

Certain computer runs involving numerical integration of the nonlinear equations, (15–20), were made to verify the results of the analytic study. The following input parameters based on the SAS-A orbital configuration were used for the cases studied: $A=C=30.895$ kg-m^2; $B=29.421$ kg-m^2; $I_{R_2}=2I_{R_1}=0.011525$ kg-m^2; $\Gamma=0.453$ m; $r_0=0.0189$ m; $r_1=0.1735$ m; $m=0.2451$kg; $s=209.4$ rad/sec, $k=5.7\times10^{-5}$ Nt-m-sec/rad; $K=5.8\times10^{-5}$ Nt-m/rad; $\omega_2(0)=0.008727$ rad/sec. The initial transverse main body rate of 0.00125 rad/sec was such that an initial system nutation angle of 0.7855° resulted. The effect of all external torques was neglected. The numerical integration step size of 0.0025 sec was selected on the basis of the high-frequency motion associated with the wheel rotation of 33.2 cps; thus for each cycle of wheel rotation approximately twelve numerical integration steps were assigned. As a result, about 60 min of IBM 360/91 computer time were required to simulate 100 sec of transient response.

The first case considered predicts the transient response of the SAS-A satellite under normal operating conditions, and with the initial wheel deflection angles and angular rates set to zero. Based on the wheel damping tests conducted at APL, the following values were selected: $K_R=71.61074$ Nt-m/rad; $k_R=6.779\times10^{-3}$ Nt-m-sec/rad. The previous analysis predicted that this system is stable with a theoretical nutation angle decay time constant of about 22 min.

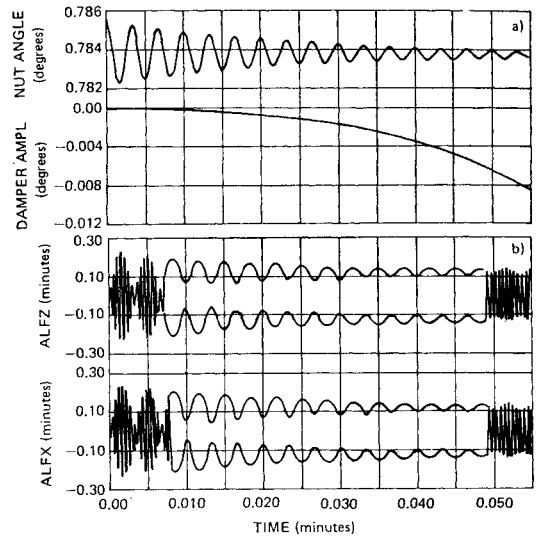

Fig. 5 Initial transient response SAS-A, damping on both main spacecraft and wheel.

Figure 5 illustrates the first 0.055 min of transient response, showing the motion of the system nutation angle, the nutation damper displacement (Fig. 5a), and the two components of momentum wheel deflection angles (Fig. 5b). Although definitive conclusions regarding stability can not be made on the basis of so short a response time, it should be noted that the wheel flexural motions never exceed an amplitude of 0.25 min of arc, and are typical of the motion simulated during the 100 sec response. The motion of both α_x and α_z as shown compares qualitatively with the results of the SAS-A wheel damping tests.

The transient response for the nominal SAS-A spacecraft over 100 sec is illustrated in Figs. 6a and 6b. In Fig. 6a it

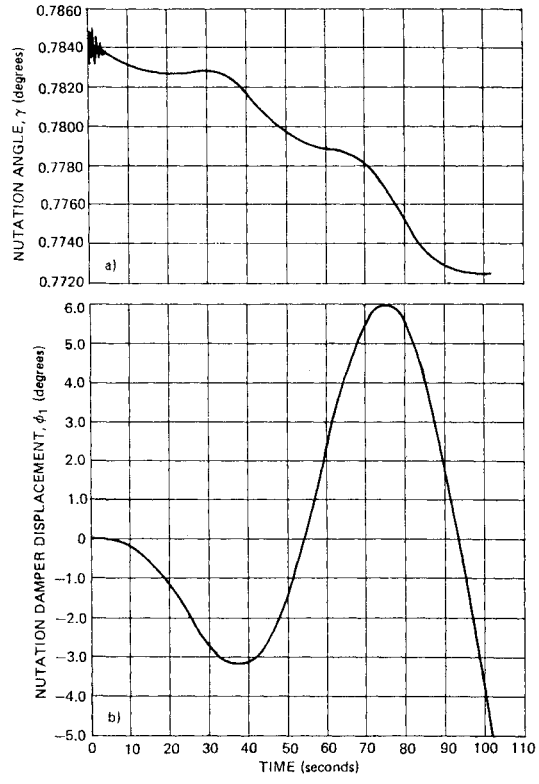

Fig. 6 Transient response SAS-A, damping on both main spacecraft and wheel.

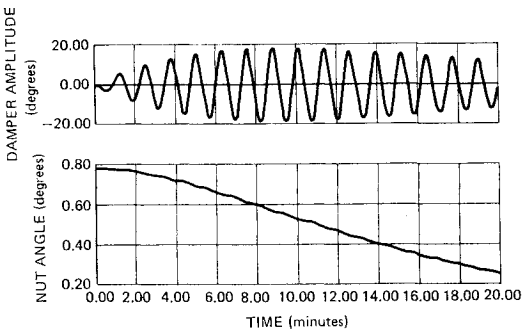

Fig. 7 Transient response SAS-A, nutation damping on main spacecraft only.

can be seen that the high-frequency component in the nutation angle response is quickly removed. The nutation angle amplitude decreases to a value of 0.7725° after 100 sec; this initial average decay rate is only one third of that theoretically predicted. Figure 6b illustrates the displacement of the pendulous nutation damper during the 100 sec.

Although stability has been verified, the following question remains. Can the increase in the nutation angle time constant be attributed to the wheel flexure dynamics? To resolve this, the case considered in Figs. 5 and 6 was rerun with the wheel flexural dynamics removed and damping only on the main body. A careful examination of these results (Fig. 7) indicated that during the first 1.67 min the response of the damper and nutation angle is similar to the results shown in Fig. 6. The rate of change of nutation angle during the first 2 min is essentially the same as that observed in Fig. 6a.

The second case considered assumes that there is no damping on the main part of the satellite, and that $k_R = 0.2$ Nt-m-sec/rad. The analysis predicts that the system is unstable, with a theoretical nutation angle time constant (exponential growth) of approximately 6000 sec. In the simulation the effect of the nutation damper and of all its coupling terms was removed. The growth of the nutation angle response is illustrated in Fig. 8. After 100 sec the nutation angle is predicted to be 0.7884 degree.

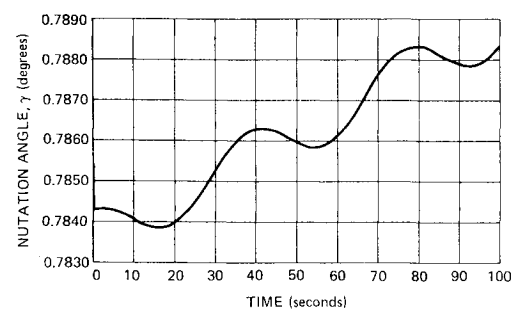

Fig. 8 Transient response SAS-A, wheel damping only.

Conclusions

As a result of the present stability analysis and numerical results the following conclusions can be made:

1) The stability criteria obtained for this system by means of averaging the "first-order" perturbations on the system nutation angle can be reduced to the criteria emanating from Likins' energy sink analysis. The implication is that higher order terms would have to be included in the averaging process to yield more complete stability information.

2) In the absence of wheel damping, some (but not all) of the previously derived Routh-Hurwitz necessary and sufficient conditions can be obtained from the present analysis.

3) A numerical evaluation of the analytical stability criterion developed here, using SAS-A satellite parameters and measured wheel damping data, indicates that system stability is insured by a factor of 128 under the normal operating conditions. The system is also stable at smaller values of rotor spin rate, although the margin of stability is somewhat reduced. If there is no damping on the despun part, but energy dissipation in the wheel, the system is unstable.

4) The time constant associated with nutation angle decay under the normal SAS-A operating conditions is 22.3 min, and is not appreciably degraded by the measured energy dissipation in the wheel.

References

[1] Bainum, P. M., Fuechsel, P. G., and Mackison, D. L., "Motion and Stability of a Dual-Spin Satellite with Nutation Damping," *Journal of Spacecraft and Rockets*, Vol. 7, No. 6, June 1970, pp. 690–696; also TG-1072, June 1969, Applied Physics Lab., The Johns Hopkins Univ., Silver Spring, Md.

[2] Mingori, D. L., "Effects of Energy Dissipation on the Attitude Stability of Dual-Spin Satellites," *AIAA Journal*, Vol. 7, No. 1, Jan. 1969, pp. 20–27.

[3] Sen, A. K. and Fleisher, G., "On the Attitude Stability of the SAS-A Spacecraft," Rept. 204 (Revised), Feb. 18, 1970, Stabilization and Control Branch, NASA Goddard Space Flight Center, Greenbelt, Md.

[4] Tossman, B. E., "Variable Parameter Nutation Damper for SAS-A," *Journal of Spacecraft and Rockets*, Vol. 8, No. 7, July 1971, pp. 743–746.

[5] Likins, P. W., Tseng, G.-T., and Mingori, D. L., "Stable Limit Cycles Due to Nonlinear Damping in Dual-Spin Spacecraft," *Journal of Spacecraft and Rockets*, Vol. 8, No. 6, June 1971, pp. 568–574.

[6] Whittaker, E. T., *A Treatise on the Analytical Dynamics of Particles and Rigid Bodies*, 4th ed., Cambridge University Press, Cambridge, England, 1959, pp. 41–44.

[7] Flatley, T. W., "Equilibrium States for a Class of Dual-Spin Spacecraft," TR-R-362, March 1971, NASA.

[8] Likins, P. W., "Attitude Stability Criteria for Dual-Spin Spacecraft," *Journal of Spacecraft and Rockets*, Vol. 4, No. 12, Dec. 1967, pp. 1638–1643.